



Fermi National Accelerator Laboratory

FERMILAB-Conf-92/280

Hyperon Properties and Magnetic Moments

Regina A. Rameika

*Fermi National Accelerator Laboratory
P.O. Box 500, Batavia, Illinois 60510*

October 1992

Presented at the *XII International Conference on Physics in Collision*,
Boulder, Colorado, June 10-12, 1992

Disclaimer

This report was prepared as an account of work sponsored by an agency of the United States Government. Neither the United States Government nor any agency thereof, nor any of their employees, makes any warranty, express or implied, or assumes any legal liability or responsibility for the accuracy, completeness, or usefulness of any information, apparatus, product, or process disclosed, or represents that its use would not infringe privately owned rights. Reference herein to any specific commercial product, process, or service by trade name, trademark, manufacturer, or otherwise, does not necessarily constitute or imply its endorsement, recommendation, or favoring by the United States Government or any agency thereof. The views and opinions of authors expressed herein do not necessarily state or reflect those of the United States Government or any agency thereof.

HYPERON PROPERTIES AND MAGNETIC MOMENTS

Regina A. Rameika
Fermi National Accelerator Laboratory
Batavia, Illinois 60510

Since the mid 1970's Fermilab has supported a continuously evolving program of experiments to study the production and decays of hyperons. Beginning with the measurements of the neutral hyperon production cross sections through the most recent experiment to measure the Ω^- 's this series of experiments has lead to both precision measurements of fundamental quantities such as magnetic moments and lifetimes as well as to the yet un-understood phenomena of hyperon polarization.¹¹ (see Table 1.) Fermilab has been an ideal place to explore the hyperon sector. Typically the hyperons are produced by protons incident on nuclear targets such as beryllium or copper, though the diversity of beams and targets available at Fermilab has allowed experiments to be done with pion and kaon beams and using targets ranging from hydrogen to lead. At the high energy available at Fermilab, hyperon production is copious, and decay lengths on the order of meters.

Table 1

Hyperon Physics @ FNAL

1974-76	E8	300 GeV	cross-sections elastic scattering $P_{\Lambda}; \mu_{\Lambda}; \mu_{\Xi^0}$
1977	E440	400 GeV	$P_{\Lambda}; \mu_{\Lambda}$
1977	E441	400 GeV	$P_{\Lambda}; \mu_{\Lambda}; \mu_{\Xi^0}$
1978	E495	400 GeV	P_{Λ} from H_2 target
1979	E361	400 GeV	Λ_b decay
1979	E620	400 GeV	$P_{\Xi^-, \Sigma^-, \Sigma^+} \rightarrow \mu_{\Xi^-, \mu_{\Sigma^-}, \mu_{\Sigma^+}}$
1980	E497	400 GeV	$P_{\Xi^-, \Sigma^-, \Sigma^+} \rightarrow \mu_{\Xi^-, \mu_{\Sigma^-}, \mu_{\Sigma^+}}$
1982	E555	400 GeV	P_{Λ} at high p_t
1982	E619	400 GeV	$\mu_{\Sigma^0 \rightarrow \Lambda}$
1984	E715	400 GeV	$\Sigma^- \beta$ -decay
1987	E756	800 GeV	$P_{\Xi^-} P_{\Omega^{(?)}} \rightarrow \mu_{\Xi^-}, \mu_{\Omega^-}$
1990	E761	800 GeV	$\Sigma^+ \rightarrow p$ γ asymmetry
1991	E800	800 GeV	$P_{\Omega^+} \rightarrow \mu_{\Omega^-}$

Additionally, the experiments are "clean". This is because the experiments focus on inclusive production in a closed geometry environment making the hyperons' simple decay topologies easy to reconstruct. The key feature in creating this environment is the use of a brass or tungsten collimator imbedded in a high field sweeping magnet. The combination of an incident production angle and the sweeping field is used to move the incident proton beam away from a defining aperture which creates the hyperon beam. The sweeping field which also removes the

low energy particles from the hyperon beam is also used to momentum select charged hyperons.

In 1976, in the midst of studying inclusive strange particle production using the Fermilab 300 GeV proton beam, it was discovered that the Λ hyperons produced at a non-zero production angle had a significant polarization which appeared to increase linearly with transverse momentum (p_t). Subsequent experiments both at Fermilab and at other accelerators confirmed this discovery in Λ 's and other hyperons.^{2]} Throughout the next decade, measurements of the polarization as a function of energy, p_t and Feynmann x (x_f) revealed that the polarization had remarkably simple behavior, though totally unpredictable by theory.

Parity conservation in the strong interaction requires that the polarization vector at production be parallel to the normal to the production plane. In the laboratory the polarization of a hyperon can be measured by analyzing the parity violating decay of the parent into a baryon and a meson. For a spin 1/2 hyperon such as a Λ , which decays to a spin 1/2 proton and a spin 0 π^- , the decay distribution of the daughter protons is given by

$$dN / d(\cos\Theta) = 1 + \alpha P \cos\Theta \quad (1)$$

Θ is the angle between the proton and the polarization direction in the rest frame of the Λ . α is the decay asymmetry parameter which describes the magnitude of the weak asymmetry in the decay, and P is the magnitude of the Λ polarization. In the case where all decay protons are detected and measured, the distribution in Equation (1) is simply a straight line which has a slope αP . In practice, experiments have less than full acceptance due to the apparatus geometry and reconstruction inefficiencies. A typical apparatus layout and event topology is shown in Figure 1. It should be

noted that Equation (1) measures the product αP . Therefore, in a case where the parent hyperon may be polarized but the decay asymmetry is small, measuring the polarization can be quite difficult. An example of this is the Σ^- hyperon where $\alpha = -0.007$. This problem can be overcome for hyperons which have a cascade decay such as a $\Xi^{0,-}$ or an Ω^- , where the parent decays to a spin 1/2 daughter, which then also decays to a spin 1/2 daughter. For the Ξ decays, the Ξ polarization is related to the Λ polarization by:

$$P_\Lambda = \frac{\gamma_\Xi P_\Xi + [\alpha_\Xi + (1 - \gamma_\Xi) \hat{\Lambda} \cdot P_\Xi] \hat{\Lambda}}{1 + \alpha_\Xi \hat{\Lambda} \cdot P_\Xi} \quad (2)$$

and for the Ω^-

$$P_\Omega = \frac{2(J+1)}{1 + \gamma_\Omega(2J+1)} P_\Lambda \quad (3)$$

where $J=3/2$ is taken as the spin of the Ω^- .^{3]}

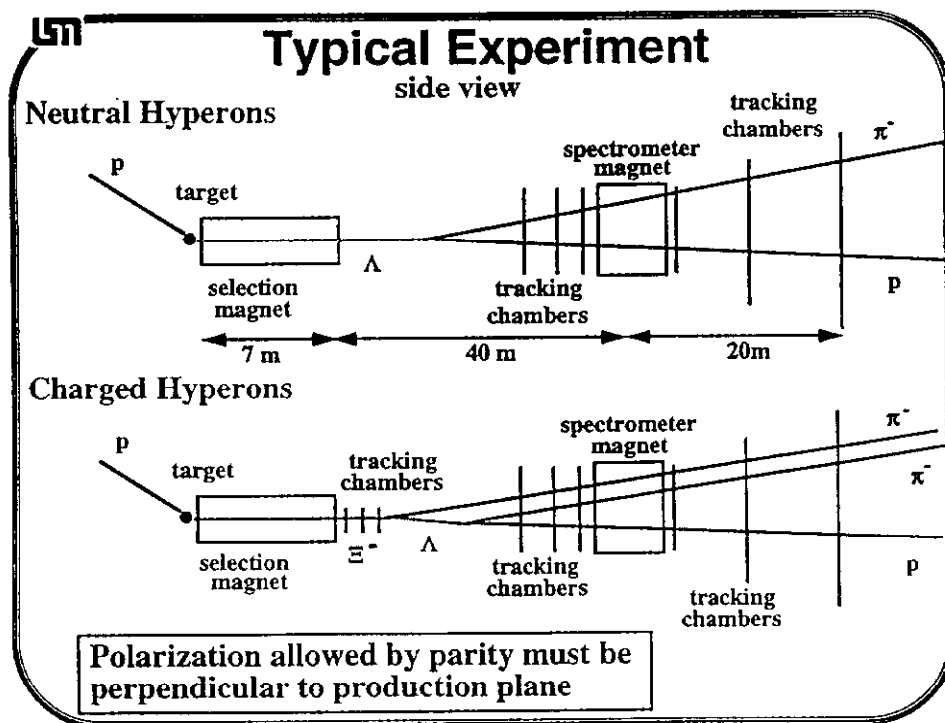


Figure 1: A typical apparatus layout and event topology.

A slight complication to the measurement of hyperon polarization is the fact that although the production polarization is normal to the production plane, the sweeping field, which is essential to the creation of the clean hyperon beam, can also precess the polarization due to the particle's magnetic moment. In the typical experiment, the proton beam is incident on the target in the y-z plane which then requires that the polarization vector lie along +/-x. The magnetic field which is usually along the y direction will then cause the polarization vector to precess in the x-z plane. This precession is illustrated in Figure 2. This complication is actually a welcomed one which has lead to one of the major successes of the hyperon program being described here. By precisely measuring the precession angle, the particle's magnetic moment can be determined. The relationship between the precession angle and the magnetic moment can be derived using simple expressions based on classical physics.

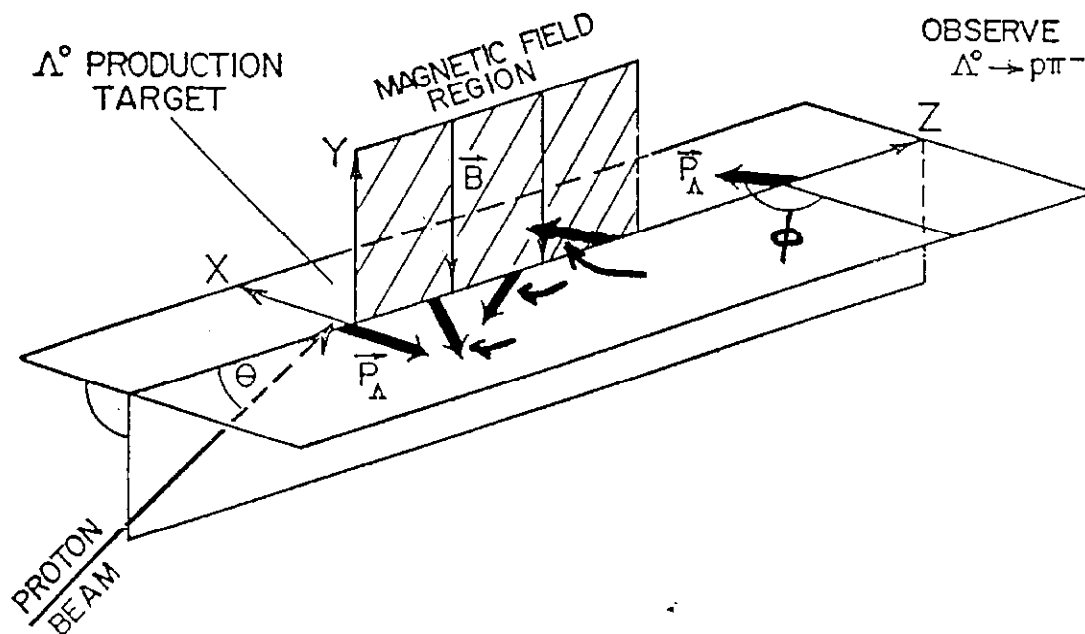


Figure 2: Precession of the polarization vector through the magnetic field.

In classical physics, a particle with **charge** q , mass m and orbital angular momentum \vec{L} , placed in an external magnetic field \vec{B} , experiences a torque which changes its angular momentum ($\vec{\tau} = d\vec{L}/dt$) according to the equation of motion

$$d\vec{L}/dt = (q/2mc) \vec{L} \times \vec{B} \quad (4)$$

The quantity $(q/2mc)\vec{L}$ is defined to be the orbital magnetic moment $\vec{\mu}_L$.

In quantum mechanics, intrinsic angular momentum, or spin S , also interacts with an external field such that

$$d\vec{S}/dt = \vec{\mu} \times \vec{B} \quad (5)$$

where $\vec{\mu}$ is the particle's intrinsic magnetic moment, defined by

$$\vec{\mu} = g/2 q/mc \vec{S} \quad (6)$$

Using Equation 6, Equation 5 can be written

$$d\vec{S}/dt = -(g/2)(q/mc) \vec{B} \times \vec{S} \quad (7)$$

This says that the spin will precess with a frequency

$$\vec{\omega}_L = -(g/2)(q/mc) \vec{B} \quad (8)$$

This is called the Larmor precession frequency. It is important to note that this is a precession measured in the rest system of the particle, and B is the magnetic induction measured in that frame.

The time rate of change of spin, measured with respect to a set of axes fixed in the lab, will be related to the rate of change of the spin in the rest system by

$$d\vec{S}/dt(\text{lab}) = d\vec{S}/dt(\text{r.s.}) + \vec{\omega} \times \vec{S} \quad (9)$$

Because the acceleration is perpendicular to the particle velocity, $\vec{\omega}$ is the Thomas precession

$$\vec{\omega}_T = \{\gamma/(\gamma+1)\}(1/c^2) \vec{a} \times \vec{v} \quad (10)$$

where \vec{a} and \vec{v} are the particle acceleration and velocity. $\beta = |\vec{v}|/c$ and $\gamma = (1 - \beta^2)^{1/2}$. For $\vec{a} = q/\gamma mc \vec{v} \times \vec{B}$, and $\vec{v} \perp \vec{B}$,

$$\vec{\omega}_T = (\gamma+1)/\gamma(q/mc) \vec{B} \quad (11)$$

Relating the proper time and magnetic induction in the rest frame, to the time and induction measured in the lab gives

$$d\vec{S}/dt(\text{lab}) = -(g/2)(q/mc)\vec{B} \times \vec{S} + \{\gamma + (1/\gamma)\}(q/mc) \vec{B} \times \vec{S}. \quad (12)$$

For $\vec{B} \perp \vec{S}$ and

$$d|\vec{S}|/dt = (1/S) d\phi/dt, \quad (13)$$

$$d\phi/dt(\text{lab}) = -q/mc (g/2 - 1 - 1/\gamma) B \quad (14)$$

where ϕ is the angle through which the spin rotates. Substituting $dt = dl/\beta c$ and integrating over the path length,

$$\phi (\text{lab}) = -q / \beta mc^2 (g/2 - 1 - 1/\gamma) \int \mathbf{B} \cdot d\mathbf{l} \quad (15)$$

For the momentum range of the typical hyperons produced at Fermilab (100-300 GeV) the contribution of the $1/\gamma$ term ranges from 1/2 to 1 degree. However, the momentum dependence of the precession angle can be eliminated by measuring the precession of the spin with respect to the momentum vector rather than the fixed laboratory axes. The momentum vector precesses through the angle

$$\phi (\text{momentum}) = -q / \beta \gamma mc^2 \int \mathbf{B} \cdot d\mathbf{l} \quad (16)$$

The net precession angle, measured with respect to the momentum, is then given by

$$\phi (\text{net}) = -q / \beta mc^2 (g/2 - 1) \int \mathbf{B} \cdot d\mathbf{l} \quad (17)$$

where ϕ is measured in degrees and $\int \mathbf{B} \cdot d\mathbf{l}$ in Tesla-meters. If the spin rotates in the same sense as the momentum, but at a faster rate, the quantity $(g/2 - 1)$ will be greater than zero. Likewise, if the spin precesses less rapidly than the momentum, $(g/2 - 1)$ will be negative. A similar though slightly less complicated derivation is given for neutral particles.^{4]}

Selecting the sample of hyperons which get used to make a magnetic moment measurement is a balance between maximizing the statistics of the sample and ensuring that the sample is pure and properly reconstructed. Examples of Ξ^- events, selection criteria and Monte Carlo distributions are shown in Figures 3 a - d.^{5]} Raw $\cos \Theta$ distributions for events from the same sample are shown in Figures 4 a - c. The lack of perfect acceptance is easily seen in the depletion of the $\cos \Theta$ distributions, particularly near the values of 0 and +/- 1. The problem with imperfect acceptance is

that, if uncorrected, fitting the distribution to Equation 1 can lead to a false asymmetry.

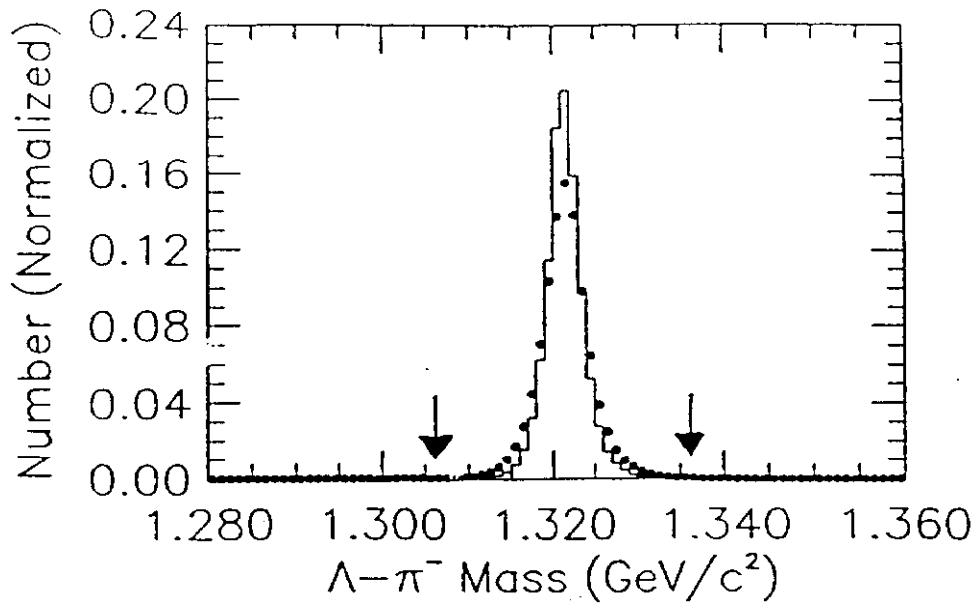


Figure 3 a: m_{Ξ^-} distribution for reconstructed data and Monte Carlo Ξ^- events. The data selection criteria is shown with an arrow. The Monte Carlo data are shown with the solid lines and the data with circles.

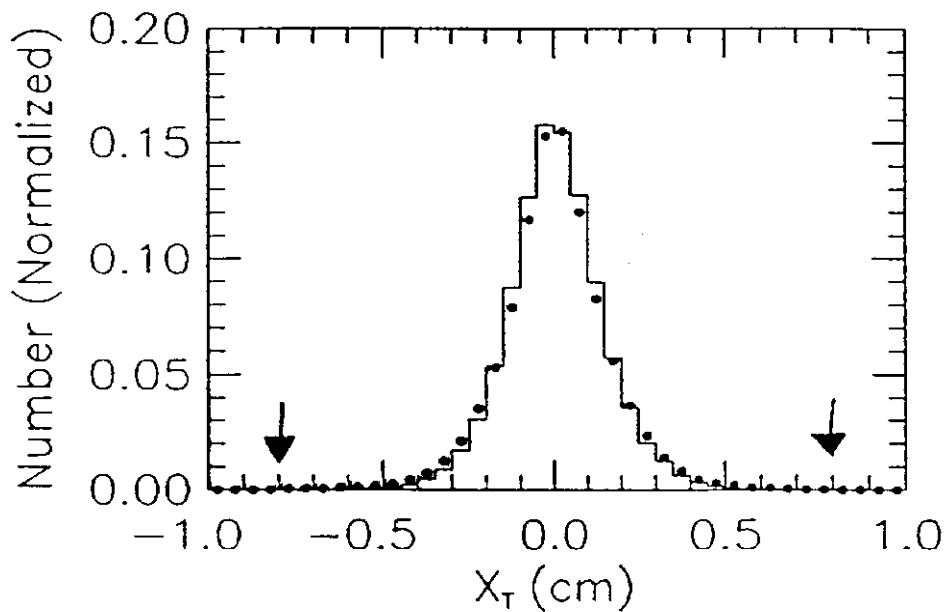


Figure 3 b: X_T (position of Ξ^- in x at the target) distribution for reconstructed data and Monte Carlo Ξ^- events. The data selection criteria is shown with an arrow. The Monte Carlo data are shown with the solid lines and the data with circles.

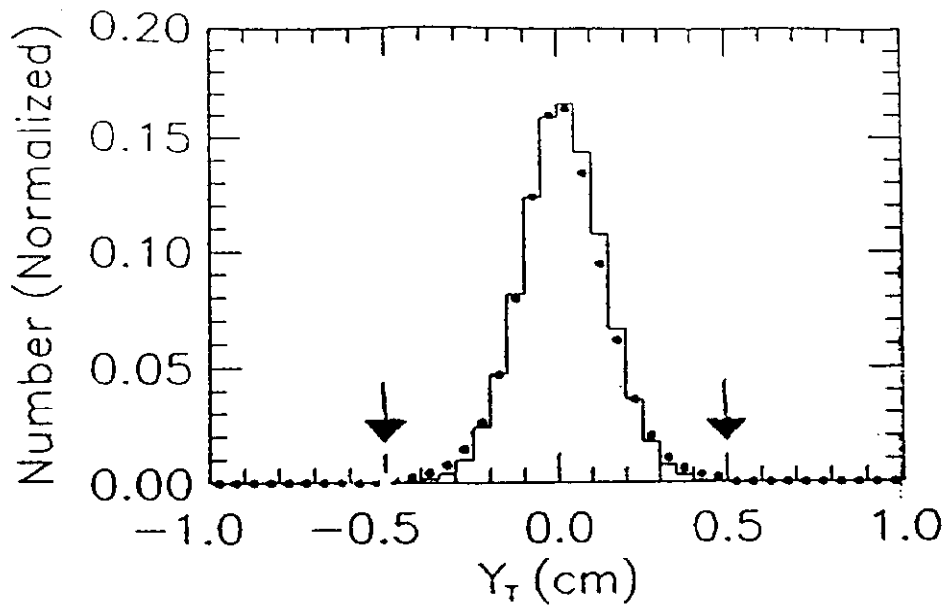


Figure 3 c: Y_T (position of Ξ^- in y at the target) distribution for reconstructed data and Monte Carlo Ξ^- events. The data selection criteria is shown with an arrow. The Monte Carlo data are shown with the solid lines and the data with circles.

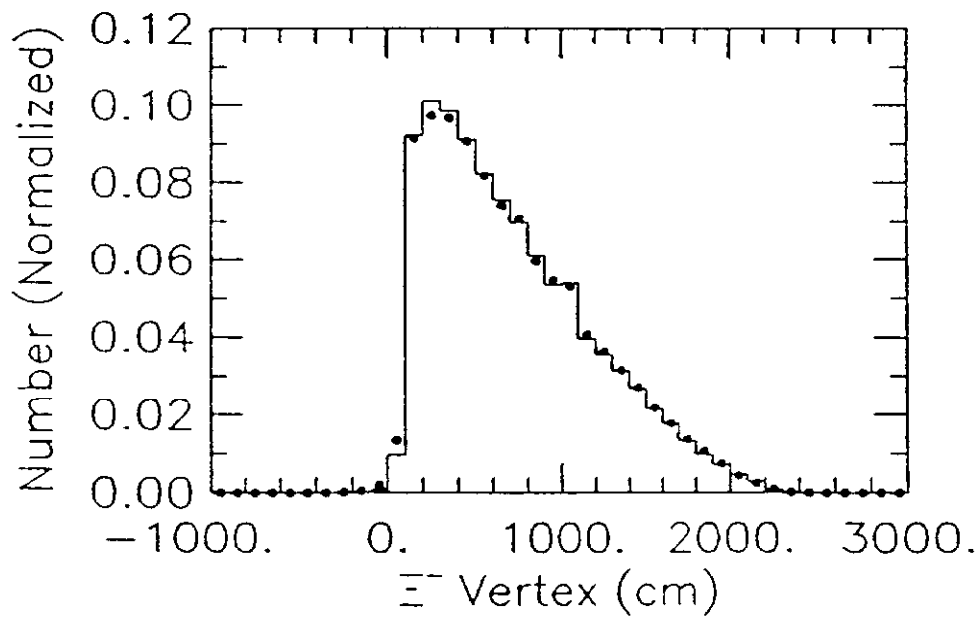


Figure 3 d: The Ξ^- vertex distribution for reconstructed data and Monte Carlo Ξ^- events. The Monte Carlo data are shown with the solid lines and the data with circles.

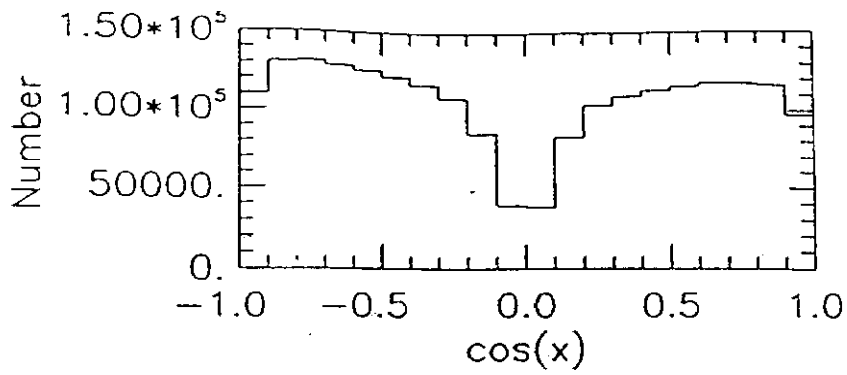


Figure 4 a

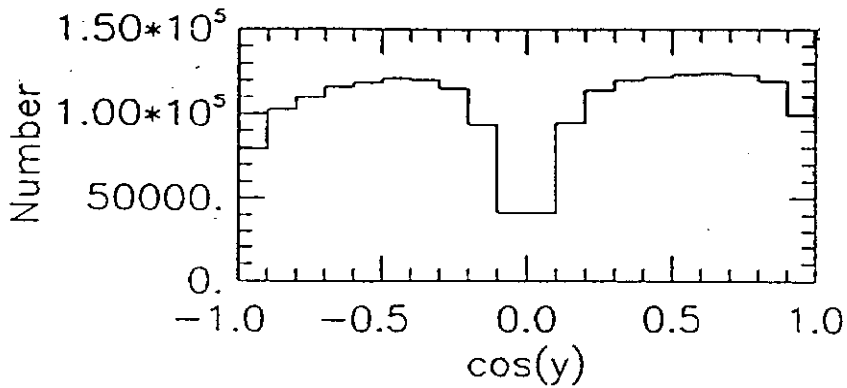


Figure 4 b

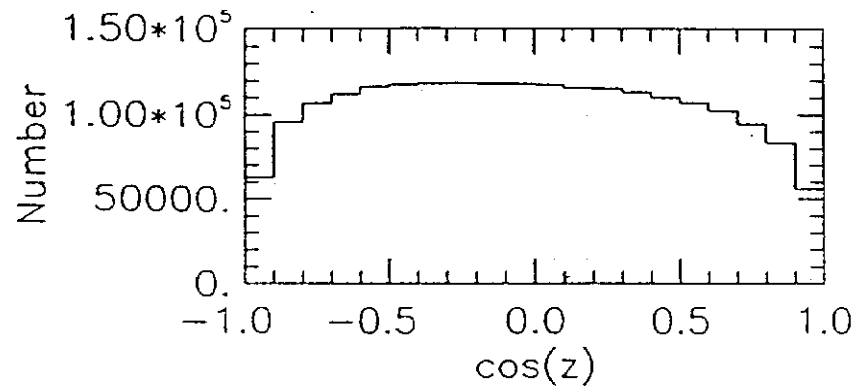


Figure 4 c

Figures 4 a - c: Raw $\cos\Theta$ (x, y, z) distributions for Ξ^- events from E756.

An experimental technique has been developed which, to first order, eliminates the problem of acceptance induced asymmetries. If the data sample has been prepared

such that a real polarization asymmetry exists, what will be measured in the $\cos \Theta$ distribution will be a "sum" of the real polarization and a bias. However, since the real polarization must be normal to the production plane, by reversing the angle of the incident proton beam, the normal to the production plane and hence the polarization is reversed. Geometrical acceptance and apparatus and software biases are unchanged by this reversal. If the total measured asymmetry is given by A then

$$A(\Theta_+) = \alpha P + B \quad (18)$$

$$A(\Theta_-) = -\alpha P + B \quad (19)$$

The bias B can be cancelled by subtracting the asymmetries taken at opposite production angles, while the sum leads to a direct measure of the bias B. The $\cos \Theta_x$ distribution for Ξ^- events taken at opposite production angles is shown in Figure 5. Clear reversal of the asymmetry can be seen.

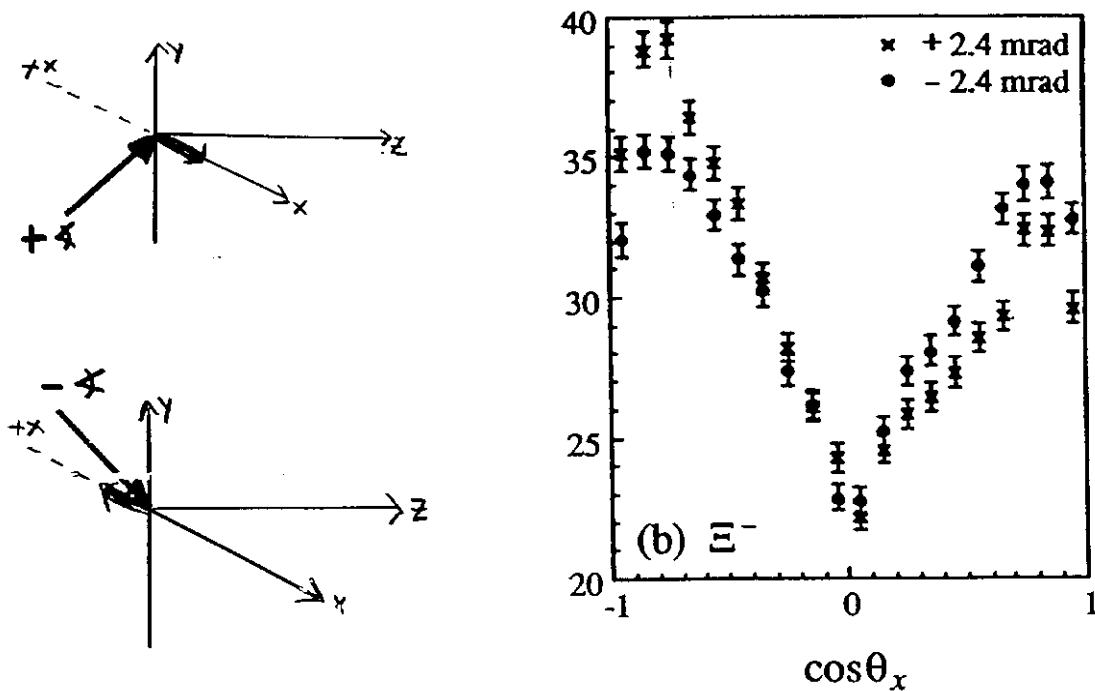


Figure 5: $\cos \Theta_x$ distribution for Ξ^- events taken at opposite production angles.

The benefit and beauty of this technique can be seen particularly well in high statistics experiments. The plots shown in Figure 6 a - f represent only a small fraction of the Ξ^- 's collected in Fermilab Experiment 756. These data were taken at the lowest value of the precession field. The signals in the x and z directions indicate that the Ξ^- 's are polarized and that the polarization vector has precessed from its initial direction along x into the x-z plane. The absence of a signal in the y direction is consistent with the requirement that parity be conserved in the strong interaction and that there are no experimental asymmetries being introduced which would produce a false signal in the y direction. The direct measurements of the biases show that the asymmetries which are not real, are small, though it can be seen that they are momentum dependent.

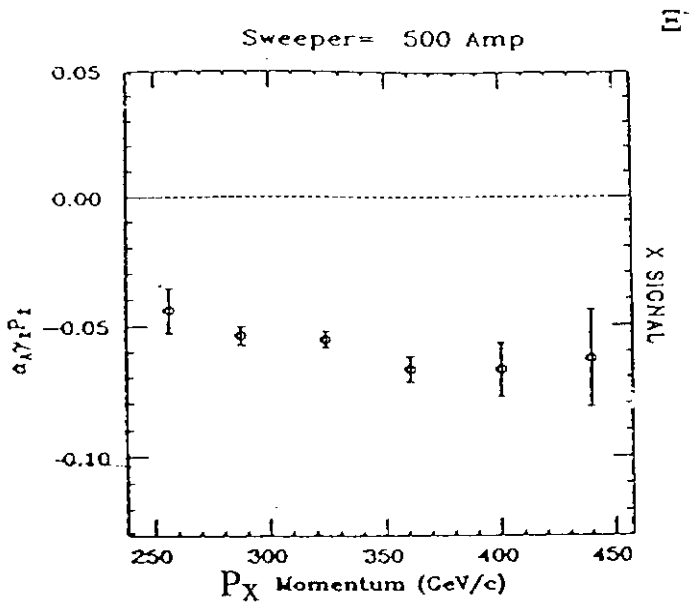


Figure 6 a

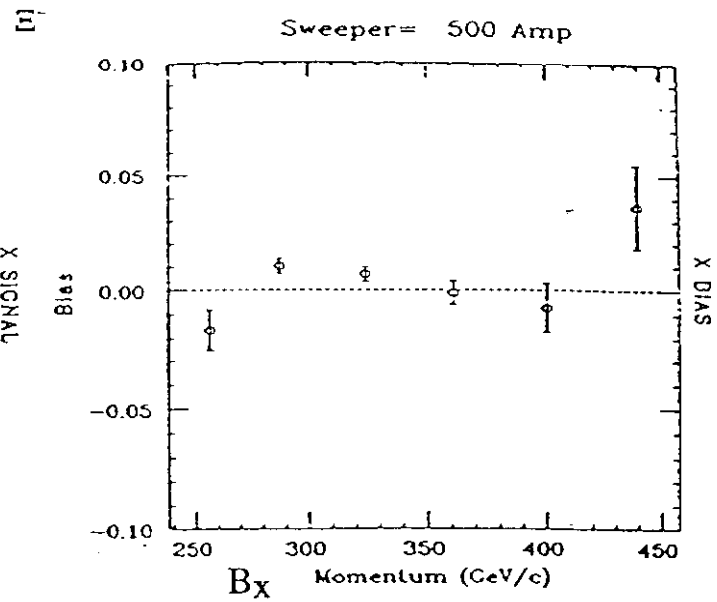


Figure 6 b

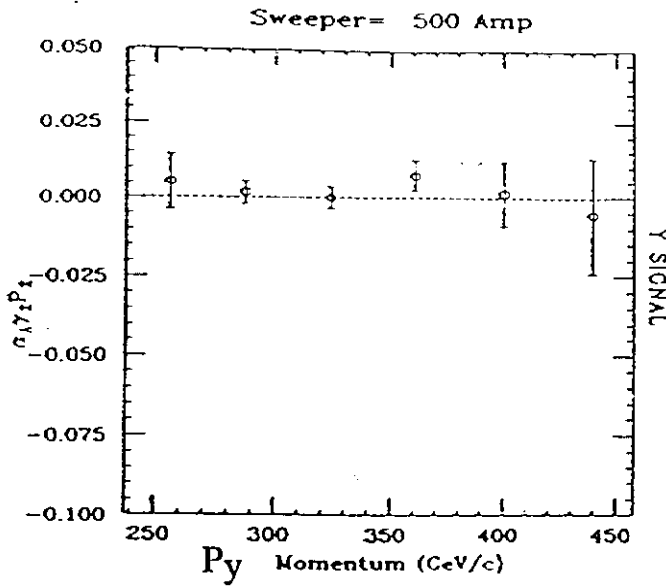


Figure 6 c

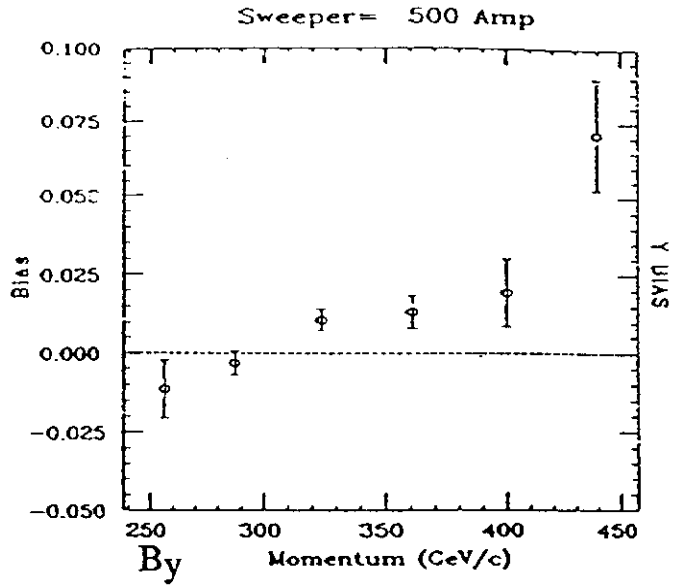


Figure 6 d

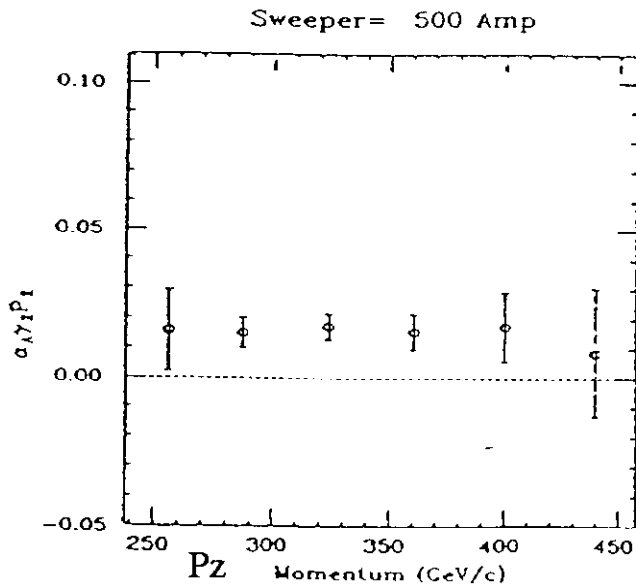


Figure 6 e

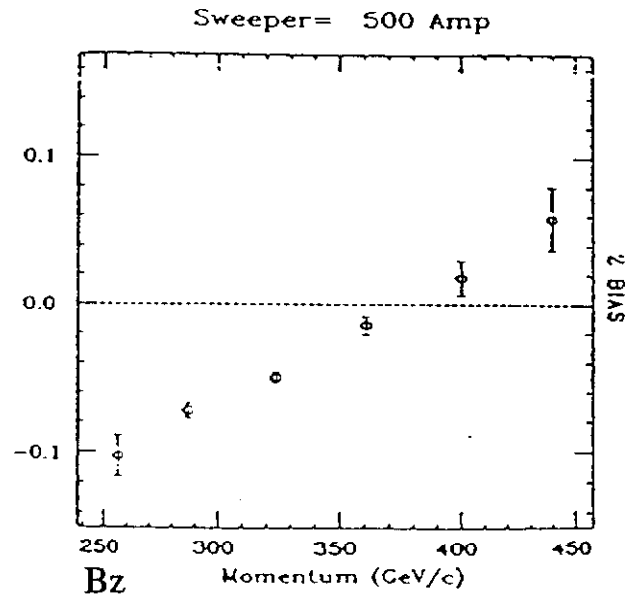


Figure 6 f

In E756 data were taken at five different values of the precession field. The polarization components along x and z were measured for each of these fields. The precession angle at each field was measured using the relationship

$$\phi = \tan^{-1}(P_z / P_x) + n\pi \quad (20)$$

Once the precession angle has been determined the magnetic moment follows from Equations 13 and 6. The error on the magnetic moment is directly proportional to the error in the precession angle and inversely proportional to the strength of the $\int B dt$. i.e.

$$\Delta g / 2 \propto \Delta \phi / \int B dt. \quad (21)$$

$\Delta \phi$ is given by:

$$\frac{P_x^2 \Delta P_x^2 + P_z^2 \Delta P_z^2}{|P|} \quad (22)$$

The variables which make up Equations 21 and 22 indicate that there are three key ingredients to making **precision** magnetic moment measurements. These are 1) making ΔP as small as possible (requires $10^5 - 10^6$ events); 2) making P as large as possible (10 to 30%) and 3) making the precession field as large as possible (10 - 25 Tesla-meters). Throughout the course of the Fermilab hyperon program success in optimizing each of these ingredients has lead to precision measurements of the Λ , Ξ^0 , Ξ^- , Σ^+ , and Σ^- magnetic moments.^{6-10]} The magnetic moment of the Ξ^- determined from the angles plotted in Figure 7 is $\Xi^- = - 0.6505 \pm 0.0025$. Similarly beautiful precession curves for the Λ^0 , Ξ^0 and the Σ^+ are shown in Figures 8 a - c. High statistics experiments like the ones described here easily allow determination of magnetic moments at the few per cent level. However, equally important to statistical precision is the understanding of the systematic errors in the measurements. While good signal to bias is one measure of the systematics, the consistency of a number like the magnetic moment as a function of momentum is also an important check. Table 2 and Figure 9 show the Ξ^- moment as a function of momentum for the full data sample.

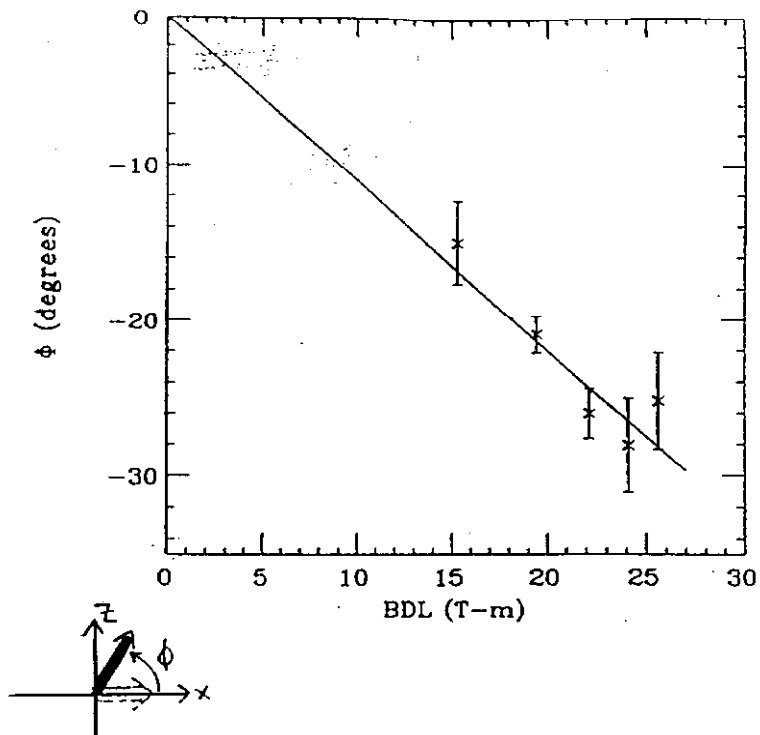


Figure 7: The magnetic moment of the Ξ^- determined from the angles plotted is $\Xi^- = -0.6505 \pm 0.0025$.

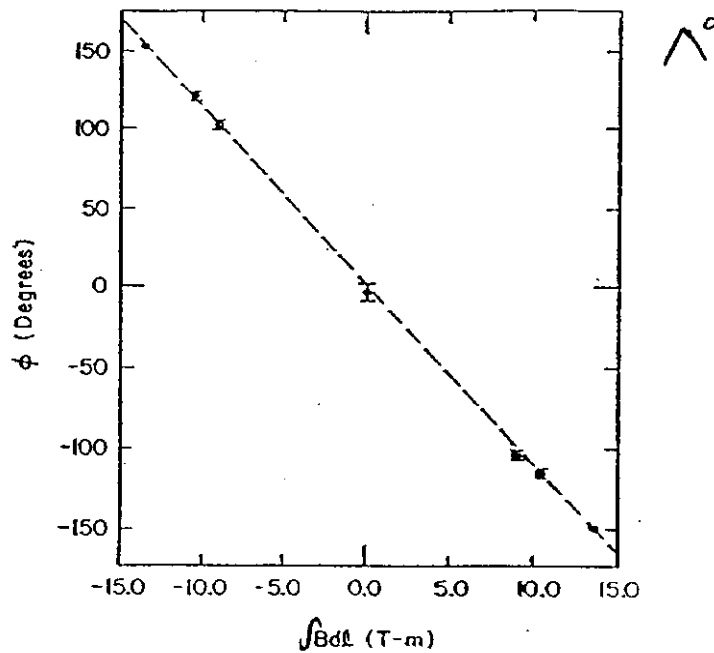


Figure 8 a: The magnetic moment of the Λ^0 determined from the angles plotted is $\mu_{\Lambda^0} = -0.613 \pm 0.004$.

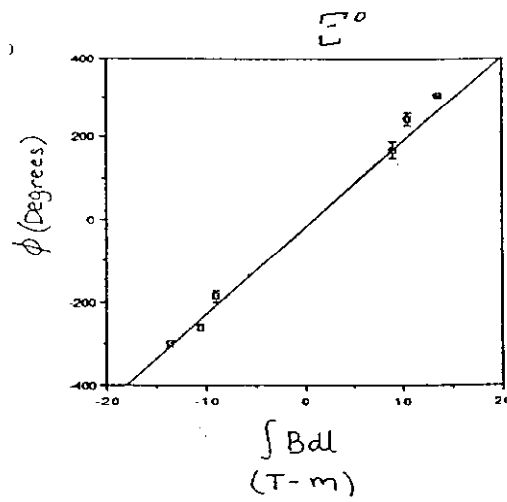


Figure 8 b: The magnetic moment of the E^- determined from the angles plotted is $\mu_{E^-} = -1.253 \pm 0.014$

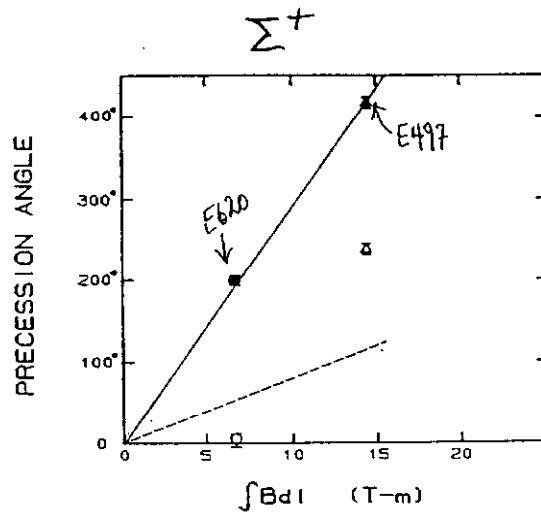


Figure 8 c: The magnetic moment of the Σ^+ determined from the angles plotted is $\mu_{\Sigma^+} = +2.379 \pm 0.020$

Table 2: μ_{E^-} as a function of momentum.

Momentum (GeV/c)	μ_{E^-} (nm)	1000's of Events
255	-0.640 ± 0.057	45
290	-0.657 ± 0.018	251
330	-0.645 ± 0.008	638
365	-0.649 ± 0.005	1025
405	-0.654 ± 0.004	1095
445	$-0.648 \pm 0.004^*$	764
480	-0.652 ± 0.006	371
520	-0.652 ± 0.010	131
560	-0.642 ± 0.020	31

$$\Delta\mu = \pm 0.0025$$

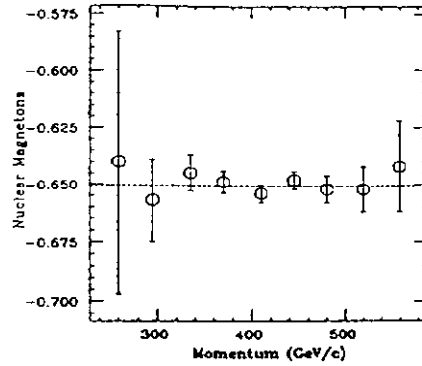


Figure 9: Ξ^- as a function of momentum

The main reason one measures the hyperon magnetic moments is to be able to compare the measurements with the theoretical predictions. Table 3 shows formulas for the hyperon moments in terms of the magnetic moments of the up, down and strange quarks. These relations are based on a simple quark model (SQM) where hyperons are described by SU(6) wave functions. Numerical predictions can be made for the hyperons if the measured values of the proton, neutron and Λ moments are used as input.

Table 3

Baryon Magnetic Moment Measurements

Baryon	Quark contribution	SQM nm
p	$\mu_p = (4/3)\mu_u - (1/3)\mu_d$	input
n	$\mu_n = (4/3)\mu_d - (1/3)\mu_u$	input
Λ	$\mu_\Lambda = \mu_s$	input
Σ^+	$\mu_{\Sigma^+} = (4/3)\mu_u - (1/3)\mu_s$	2.74
Σ^-	$\mu_{\Sigma^-} = (4/3)\mu_d - (1/3)\mu_s$	-1.21
$\Sigma^0 - \Lambda$	$\mu_{\Sigma^0 - \Lambda} = \frac{1}{\sqrt{3}}(\mu_u + \mu_d)$	-1.63
Ξ^0	$\mu_{\Xi^0} = (4/3)\mu_s - (1/3)\mu_u$	-1.46
Ξ^-	$\mu_{\Xi^-} = (4/3)\mu_s - (1/3)\mu_d$	-0.52
Ω^-	$\mu_\Omega = 3\mu_s$	-1.83

From 1978 through 1981 the evolution of the Fermilab hyperon program provided many experimental measurements so that the theoretical predictions could be tested. However one particle remained elusive - the Ω^- . For the most part this is because the Ω^- is the rarest of the hyperons, being produced only at the rate of about 1/100 of the Ξ^- . Indeed the Ω^- is an ideal particle to measure for magnetic moment studies since it is an extremely simple system - three strange quarks with aligned spins. In the SQM both μ_α and μ_λ provide direct measures of the strange quark moment. In 1981, Fermilab Experiment 620 collected a sample of 2000 Ω^- s, which were amusing but below the threshold for a statistically significant measurement of the polarization.^{11]} Coupled with the difficulty in obtaining events it was worried that producing polarized Ω^- s might not be trivial. Though polarization seemed to be a general feature of hyperon production, the anti- Λ was unpolarized up to a p_t of 2 GeV/c.^{12]} (see Figures 10 and 11) While the cross-section of Ω^- production seemed to follow the general shape of baryon production, like the anti-hyperons it contains no quarks in common with the incident proton beam. With the general lack of understanding of the polarization mechanism, whether or not Ω^- would be produced polarized remained an open question.

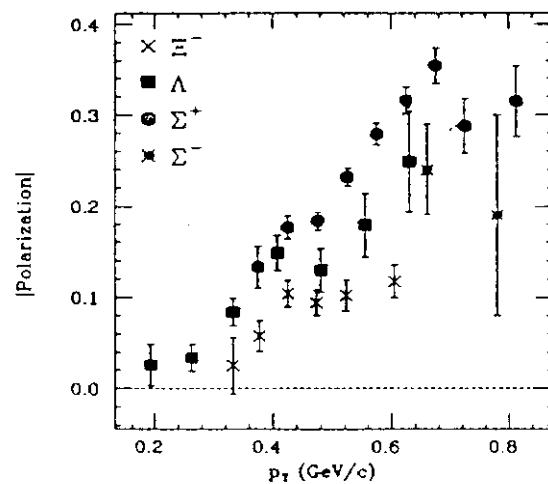


Figure 10: The magnitude of the polarization for different hyperons is remarkably similar.

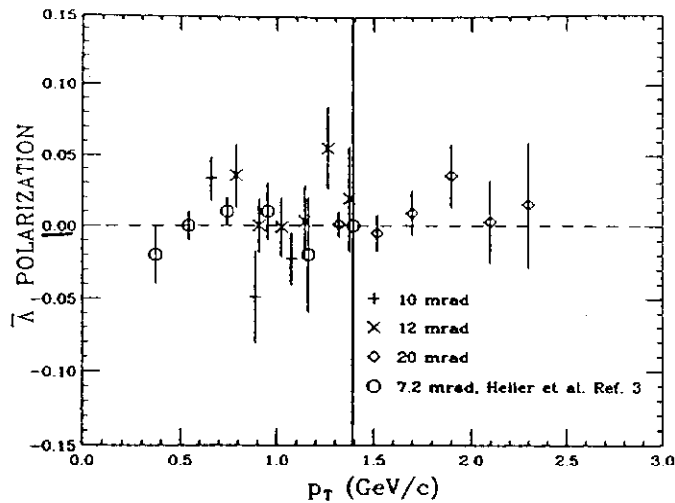


Figure 11: Anti-lambda's show no indication of polarization up to a p_T of 2 GeV/c.

In 1987, E756 answered that question. Figures 12.a - c show the polarization asymmetries measured for Ω^- 's produced with an 800 GeV proton beam.^{13]} As suspected the polarization is insignificant. This is particularly obvious when the Ω^- "polarization" is plotted in comparison to the Ξ^- and the anti- Λ , as shown in Figure 13. Not to be daunted by the mysteries of the polarization phenomena, the E756 group modified the Ω^- production method to produce the Ω^- 's using a neutral beam, composed of neutrons, Λ 's and Ξ^0 's. In this way, the Ω 's which were produced from the incident neutral hyperons, now did have quarks in common with the incident beam. Additionally, the neutral beam was produced at a 1.8 mrad production angle such that the Λ 's and Ξ^0 's were polarized along the x direction. (see Figure 14) The experiment collect 22,000 Ω s in this mode which was called "spin-transfer". The expectation was that some fraction of the neutral hyperons' polarization would transfer to the Ω 's and then precess into the x-z plane due to the Ω magnetic moment. The resulting x and z signals are plotted in Figure 15. Though the statistics are not compelling, a magnetic moment can be calculated. If the polarization is assumed real the resulting moment is $\mu_\Omega = -2.02 \pm 0.16$.^{14]}

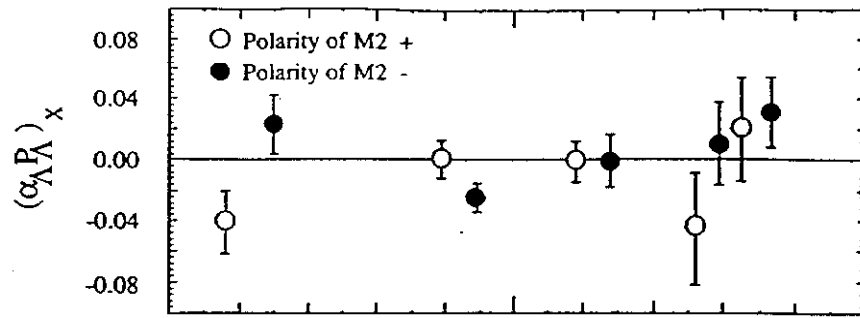


Figure 12 a: x- Polarization asymmetries for Ω^{-1} s produced by 800 GeV protons.

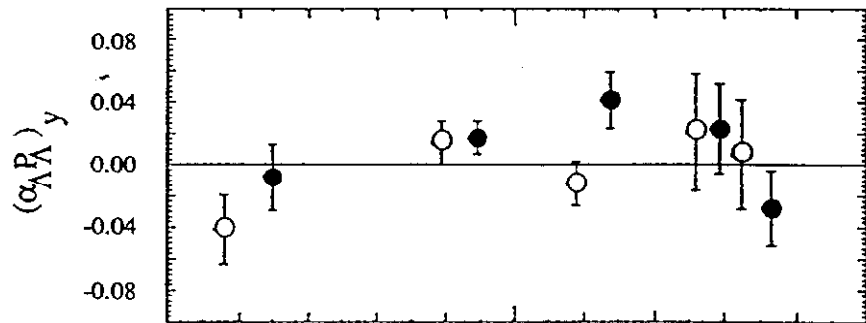


Figure 12 b: y- Polarization asymmetries for Ω^{-1} s produced by 800 GeV protons.

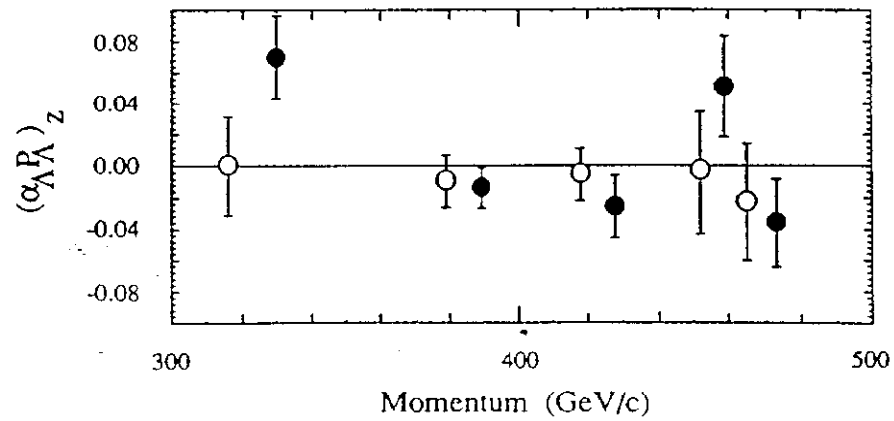


Figure 12 c: z- Polarization asymmetries for Ω^{-1} s produced by 800 GeV protons.

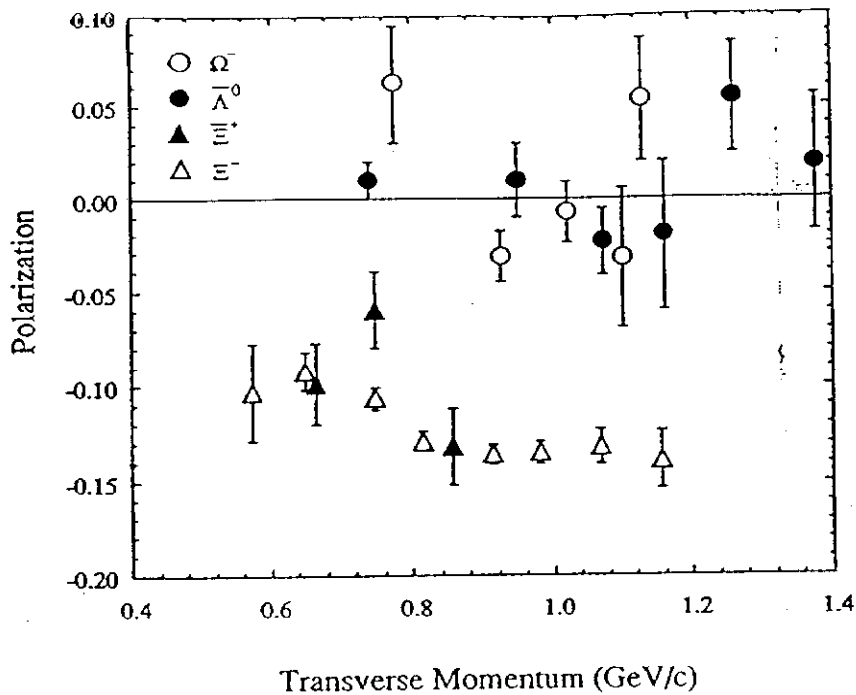


Figure 13: Ω^- "polarization" compared to other hyperons.

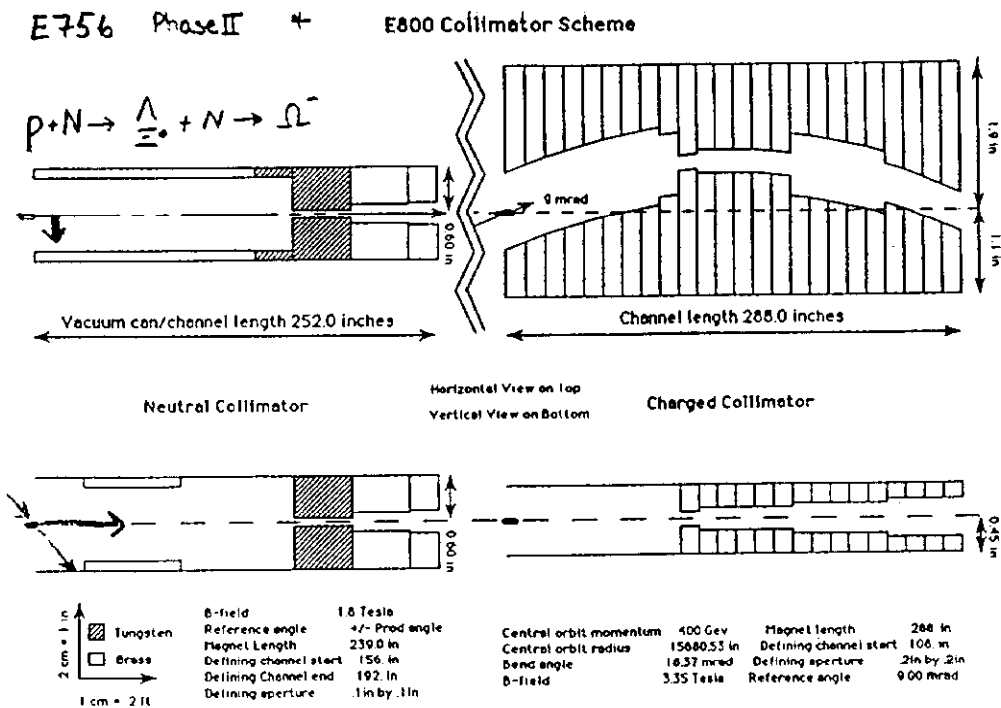
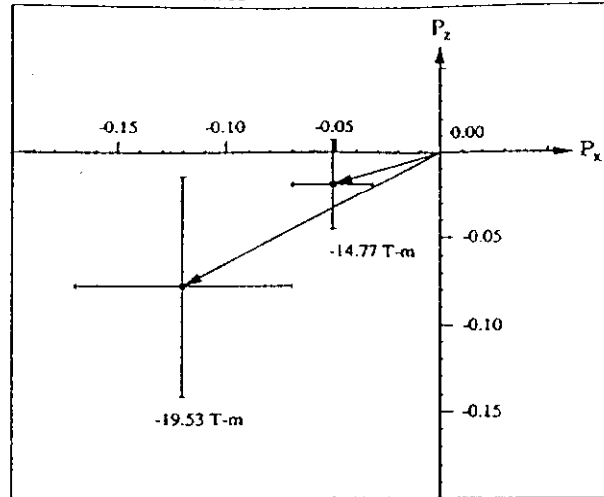


Figure 14

Figure 15: Ω^- polarization signals from E756.

A follow on experiment to E756, called E800, completed data taking in January 1992. This experiment collected a total of 400,000 Ω^- 's; approximately 50,000 in the spin transfer mode, and 150,000 in an inclusive production mode which is discussed below. The remainder were produced by protons for alignment and other studies. In the inclusive production mode the neutral beam is produced at a zero mrad production angle and so the neutral hyperons are unpolarized. They are however incident on the Ω^- production target at a non-zero production angle. Though the analysis of this data is very preliminary, both neutral beam production modes give both polarization and magnetic moment results consistent with the E756 result. A final result is expected within the year.

Table 4 shows the current status of magnetic moment measurements compared with the SQM predictions. On a coarse scale the agreement is quite good, though on the finer scale one can see that the agreement is particularly poor with the Ξ hyperons. Attempts to refine the SQM yield little improvement to the problem. This course to fine scale view is demonstrated in Figures 16a and 16b.

Table 4

Baryon Magnetic Moment Measurements

Baryon	Measurement in nuclear magnetons	Quark contribution	NQM nm
p	2.793	$\mu_p = (4/3)\mu_u - (1/3)\mu_d$	input
n	-1.913	$\mu_n = (4/3)\mu_d - (1/3)\mu_u$	input
Λ	-0.613 ± 0.004	$\mu_\Lambda = \mu_s$	input
Σ^+	2.419 ± 0.022	$\mu_{\Sigma^+} = (4/3)\mu_u - (1/3)\mu_s$	2.74
Σ^-	-1.156 ± 0.014	$\mu_{\Sigma^-} = (4/3)\mu_d - (1/3)\mu_s$	-1.21
$\Sigma^0 - \Lambda$	-1.61 ± 0.08	$\mu_{\Sigma^0 - \Lambda} = \frac{1}{\sqrt{3}}(\mu_u + \mu_d)$	-1.63
Ξ^0	-1.23 ± 0.14	$\mu_{\Xi^0} = (4/3)\mu_s - (1/3)\mu_u$	-1.46
Ξ^-	-0.6505 ± 0.0025	$\mu_{\Xi^-} = (4/3)\mu_s - (1/3)\mu_d$	-0.52
Ω^-	-2.02 ± 0.16	$\mu_\Omega = 3\mu_s$	-1.83

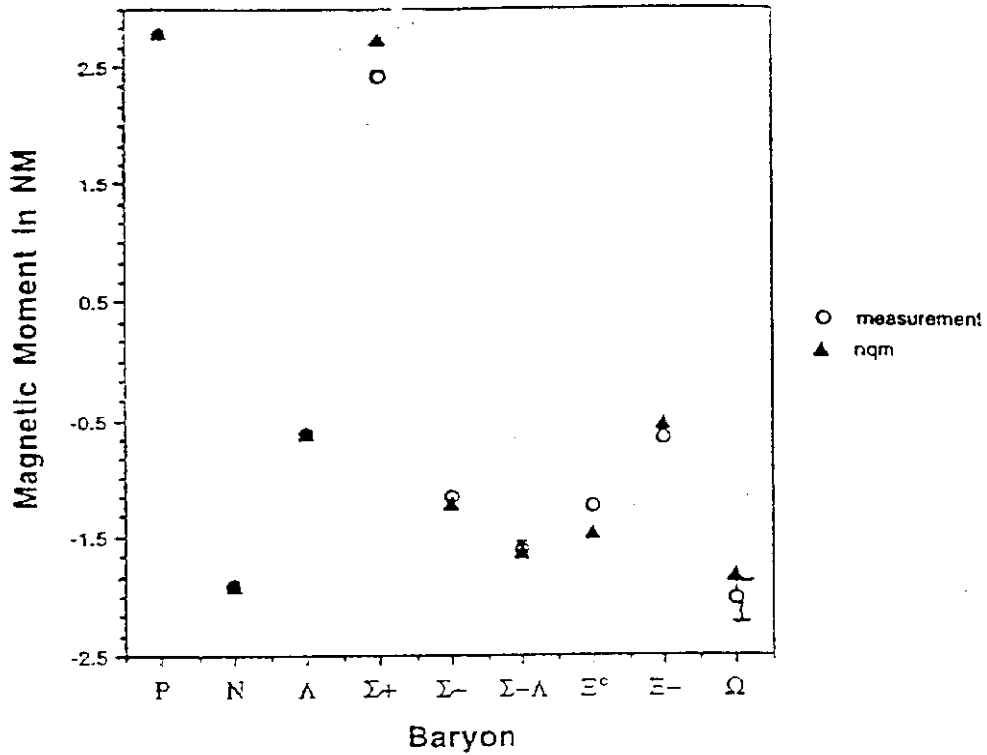


Figure 16 a: Theoretical vs. Experimental magnetic moments

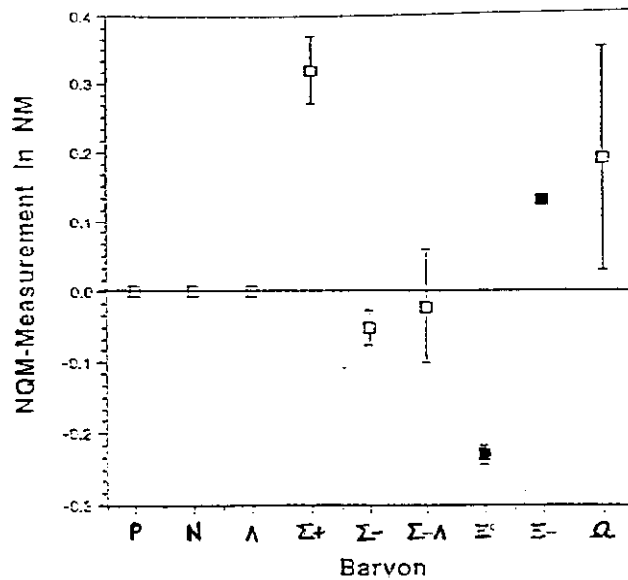


Figure 16 b: Theoretical vs. Experimental magnetic moments

An interesting twist to the hyperon polarization picture was uncovered when E756 collected a sample of 70,000 anti- Ξ^- 's. While the folklore and anti- Λ 's indicated that the anti-hyperons would be unpolarized, as were the Ω 's, it was discovered that the anti- Ξ^- had a significant polarization.^{15]} The anti- Ξ^- polarization is plotted in Figure 17 as a function of p_t , along with the signal from 400 and 800 GeV Ξ^- 's. The agreement is striking.

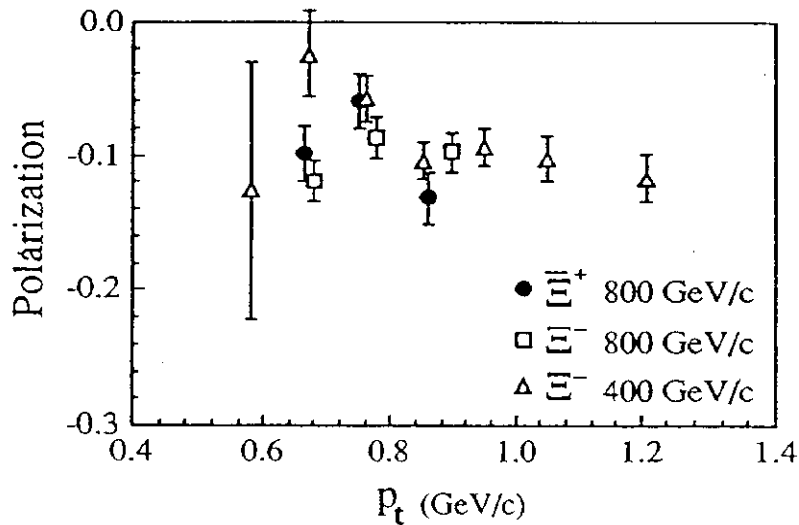


Figure 17

At this time our understanding of what causes particles to be produced polarized is more uncertain than ever. What we thought was predictable behavior is

certainly questionable with the anti- Ξ^- results. Indeed, another Fermilab hyperon experiment, E761, is analyzing a large sample of anti- Σ^- results, and has preliminary indications that yet another anti-hyperon has a non-zero polarization signal.^{16]}

Now, it is true, that excluding the anti-hyperon puzzle, some simple “theoretical” rules did seem to predict the experimental data. One idea of DeGrand and Miettinen was to use the quark model of the hyperon, where the valence quarks are those of the hyperon which are in common with the incident beam projectile, and the others are from the sea. “Sea” quarks are required to speed up to form the hyperon and are negatively polarized. “Projectile” quarks slow down to form the hyperon and are positively polarized. The polarization has the same strength in both cases, and results totally from the quark combination process.^{17]} There are other models which have the polarization coming from the quark production mechanism or both production and combination.^{18]}

The problem with most of the models, in addition to the fact that they have little real theoretical motivation, is that although they have some success in predicting the direction and magnitude of the overall polarization, they are not able to address the kinematic behavior of the effect. Experimentally, particularly for the Λ , it has been determined that the kinematic behavior is consistent with being energy independent, there is a transverse momentum plateau, such that the polarization increases with p_t up to about 1 GeV/c and then saturates, and finally, is strongly dependent on x_f . (see Figure 18)^{19]}

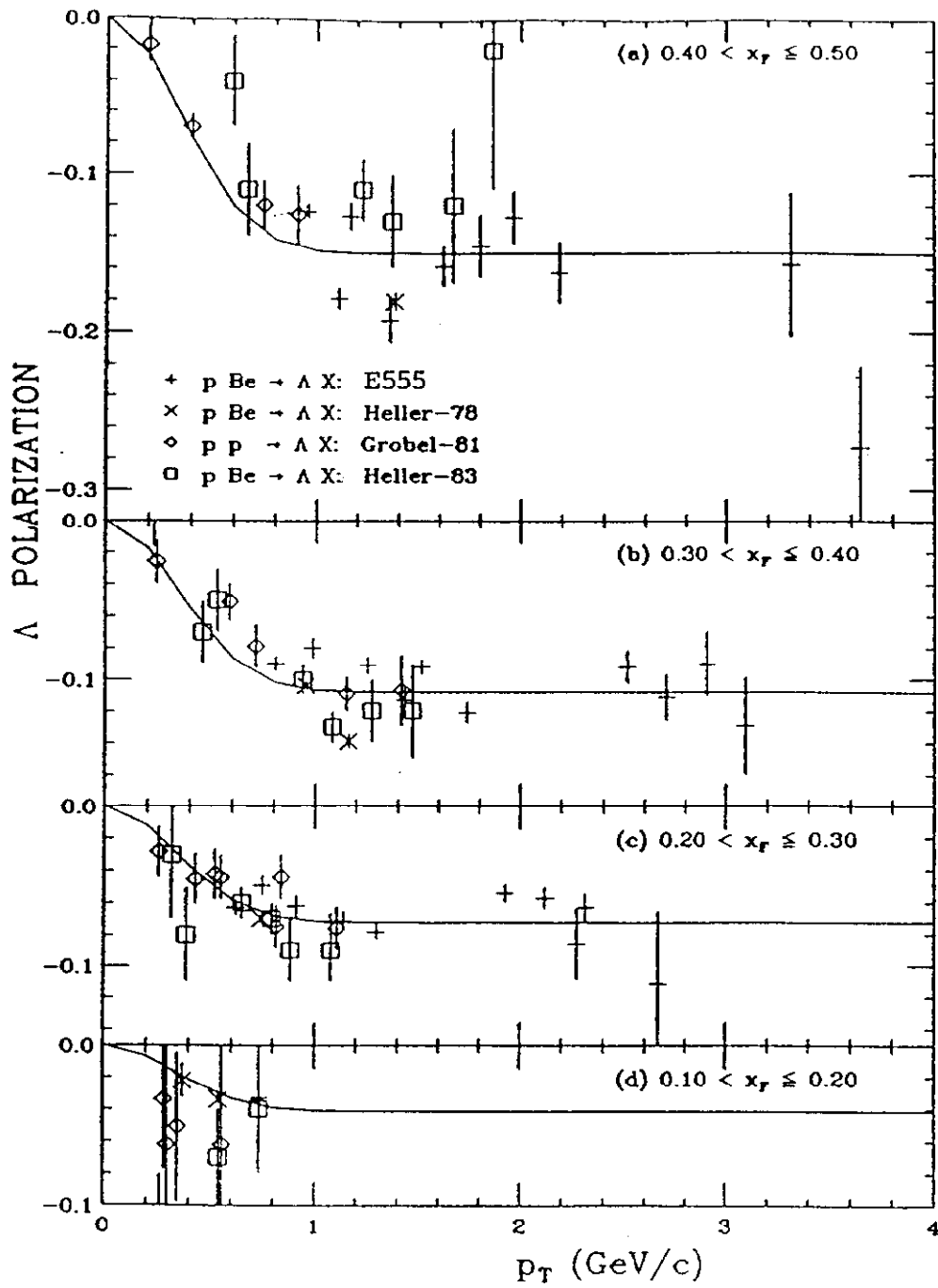


Figure 18

Collecting large samples of data for hyperons other than the Λ was not possible until the Fermilab energy increase from 400 to 800 GeV. The E756 Ξ^- data finally offered enough statistical power to begin to explore the kinematic dependence of the polarization in another particle. For better or worse, what was found was that the simple Λ rules did not hold for the Ξ^- . The striking difference between the Λ and the Ξ^- is seen in Figures 19 and 20 a-b.

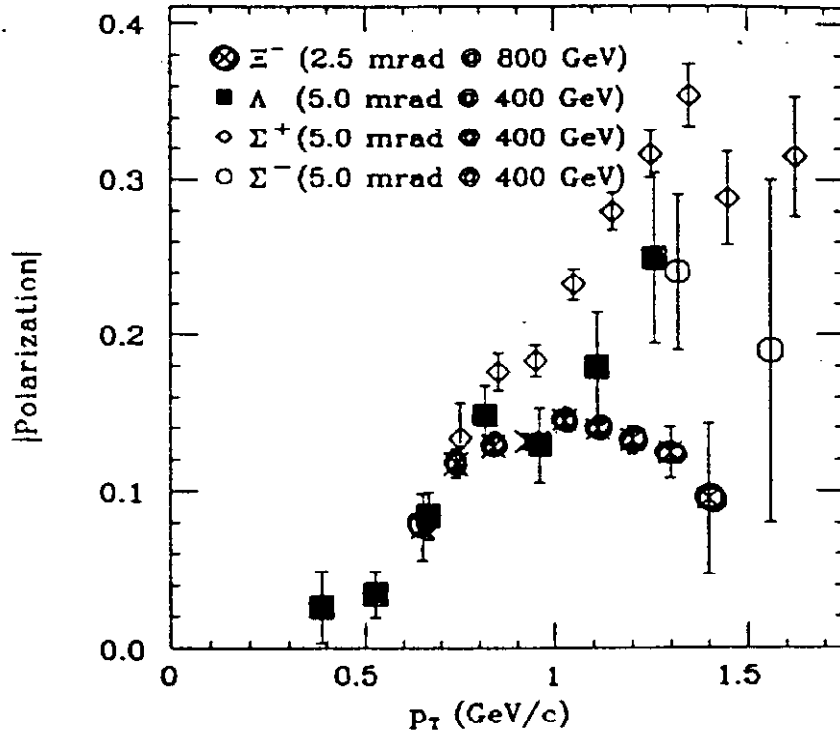


Figure 19

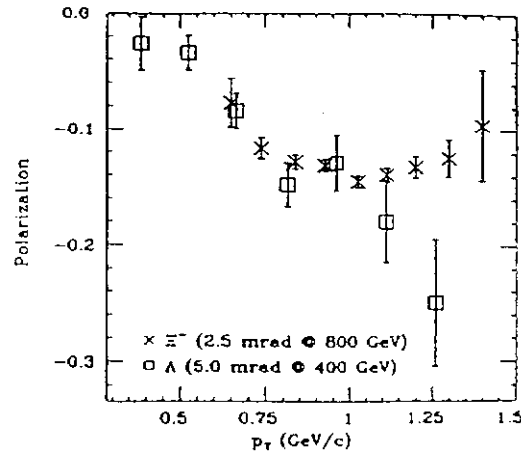


Figure 20 a

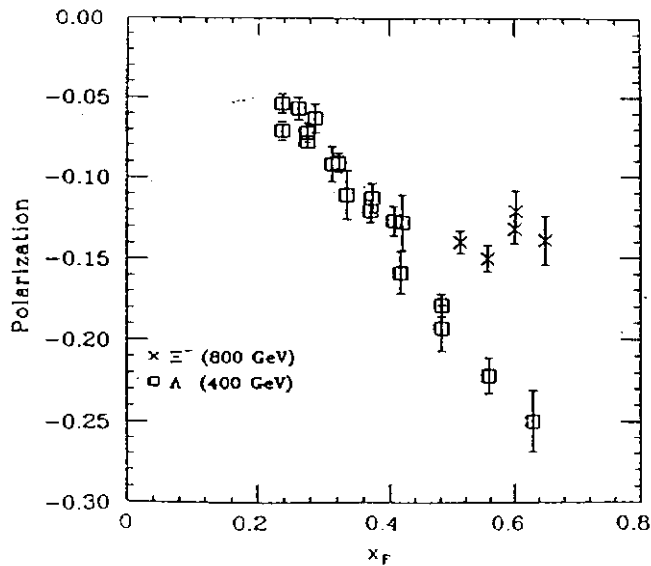


Figure 20 b

At this time the Fermilab Hyperon program is complete. Though the origin of the polarization remains unexplained, it has provided the mechanism for completing the magnetic moment measurements. Perhaps in the future, a new program could be initiated to further explore the mysteries of hyperon spin effects, though it is likely that this will have to wait for some theoretical advances to justify the experimental program. Until then we are left with the situation that spin effects which can be calculated aren't easily measured and those that we measure aren't easily calculated.

References

- 1] L. G. Pondrom, Physics Reports, Volume 122, Numbers 2 and 3, June 1985.
- 2] G. Bunce et al., Physical Review Letters, Volume 36, Number 1113, 1976; K. Heller et al., Physical Review Letters, Volume 68B, Number 480, 1977; K. Heller et al., Physical Review Letters, Volume 41, Number 607, 1978; Volume 45, Number 1043 (E), 1980; F. Lomanno et al., Review Letters, Volume 43, Number 1905, 1979; S. Erhan et al., Physical Letters, Volume 82B, Number 301, 1979; K. Raychaudhuri et al., Physical Letters, Volume 90B, Number 319, 1980; Volume 93B, Number 525 (E), 1980; F. Abe et al., Physical Review Letters, Volume 50, Number 1102, 1983; J. Phys. Soc. Jpn., Volume 52, Number 4107, 1983.
- 3] R. Handler et al., Physical Review D, Volume 25, Number 3, February 1982; K. B. Luk et al., Physical Review D, Volume 38, Number 19, 1988
- 4] See for example J. D. Jackson, Classical Electrodynamics, Chapter 11.
- 5] J. W. Duryea, Ph.D. Thesis, University of Minnesota, July 1991.
- 6] L. Schachinger et al., Physical Review Letters, Volume 41, Number 1348, 1978
- 7] P. T. Cox et al., Physical Review Letters, Volume 46, Number 14, April 1981.
- 8] J. Duryea, et al., Physical Review Letters, Volume 68, Number 6, February 1992.
- 9] C. Wilkinson et al., Physical Review Letters, Volume 58, Number 9, March 1987.
- 10] G. Zapalac et al., Physical Review Letters, Volume 57, Number 1526, 1986.
- 11] K. B. Luk et al., Physical Review D, Volume 38, Number 1, July 1988.
- 12] B. Lundberg et al., Physical Review D, Volume 40, Number 11, December 1989.
- 13] K. B. Luk, et al., Preprint VMN-Ex-1032, LBL 32409
- 14] H. T. Diehl, et al., Physical Review Letters, Volume 67, Number 7, August 1991.
- 15] P. M. Ho, et al., Physical Review Letters, Volume 65, Number 14, October 1990.
- 16] Private Communication, J. Lach, Fermilab.

- 17] T. DeGrand and H. Miettinen, Physical Review D, Volume 24, Number 2419, 1981.
- 18] P. Kroll, AIP Conference Proc. 187, High Energy Spin Physics, 1989.
- 19] B. Lundberg et al., Physical Review D, Volume 40, Number 11, December 1989.